BIOMOLECULES & THERAPEUTICS

Original Article
Biomol Ther 26(2), 182-190 (2018)

Modulation of Electroosmotic Flow through Skin: Effect of Poly(Amidoamine) Dendrimers

Hye Ji Kim and Seaung Youl Oh*

College of Pharmacy, Sookmyung Women's University, Seoul 04310, Republic of Korea

Abstract

The objective of this work is to evaluate the effect of polyamidoamine (PAMAM) dendrimers on electroosmotic flow (EOF) through skin. The effect of size and concentration of dendrimer was studied, using generation 1, 4 and 7 dendrimer (G1, G4 and G7, respectively). As a marker molecule for the direction and magnitude of EOF, a neutral molecule, acetoaminophen (AAP) was used. The visualization of dendrimer permeation into the current conducting pore (CCP) of skin was made using G4–fluorescein isothiocyanate (FITC) conjugate and confocal microscopy. Without dendrimer, anodal flux of AAP was much higher than cathodal or passive flux. When G1 dendrimer was added, anodal flux decreased, presumably due to the decrease in EOF by the association of G1 dendrimer with net negative charge in CCP. As the generation increased, larger decrease in anodal flux was observed, and the direction of EOF was reversed. Small amount of methanol used for the preparation of dendrimer solution also contributed to the decrease in anodal flux of AAP. Cross-sectional view perpendicular to the skin surface by confocal laser scanning microscope (CLSM) study showed that G4 dendrimer-FITC conjugate (G4-FITC) can penetrate into the viable epidermis and dermis under anodal current. The permeation route seemed to be localized on hair follicle region. These results suggest that PAMAM dendrimers can permeate into CCP and change the magnitude and direction of EOF. Overall, we obtained a better understanding on the mechanistic insights into the electroosmosis phenomena and its role on flux during iontophoresis.

Key Words: PAMAM dendrimer, Electroosmotic flow, Acetaminophen, Methanol, FITC

INTRODUCTION

Iontophoresis uses low electric current to increase the penetration of charged molecules mainly by electromigration. It can also enhance the passive transport of neutral molecules by changing the skin structure and lowering the barrier property of skin (Guy *et al*., 2000; Lee and Oh, 2005). One more flux enhancing effect by iontophoresis is EOF due to the net negative charge of CCP in skin at pH 7.4 (Burnette and Ongpipattanakul, 1987). Thus, current passage through CCP causes a net convective solvent flow in the anode-to-cathode direction, facilitating cation transport and inhibiting that of anions (Kim *et al*., 1993). Relative importance of electromigration and EOF depends on the physicochemical and electrical characteristics of the membrane and permeating molecule (Guy *et al*., 2000). The pH of bathing medium can change the net charge of the skin, and reverse the direction of EOF at low pH (Oh, 2011).

The application of iontophoresis using a solution or a gel, where drug molecules are simply dissolved, may be satisfactory for the therapeutic delivery in some cases. However, when the drug penetration through the skin is not enough by this method, other penetration enhancing method may also be needed in combination with iontophoresis. Dendrimers are emerging as a nanocarrier in skin drug delivery due to their small size, monodispersity, and highly functional surfaces (Sun *et al*., 2012). Among them, PAMAM dendrimer has been widely studied, due to its usefulness as a release modifier and solubilizer for hydrophobic drug molecules (Choudhary *et al*., 2017). PAMAM dendrimer is made by stepwise synthesis from core molecule, leading to a star-shaped or generational structure with nearly monodispersed molecular weight (Esfand and Tomalia, 2001; Tripathy and Das, 2013). The diameter is usually about 2-10 nm, and is similar to small proteins such as cytochrome C or hemoglobin (Esfand and Tomalia, 2001). The pKa of surface primary amine group is ~9.2 and they are cationic polyelectrolytes in pH 7.4. The pKa for the interior tertiary amine group of G4-NH_2 dendrimers is ~6.3 (Niu *et al*., 2003). The well-defined structural characteristics of dendrimers and

Open Access **https://doi.org/10.4062/biomolther.2017.203**

Received Oct 12, 2017 **Revised** Oct 17, 2017 **Accepted** Oct 19, 2017
Published Online Jan 9, 2018

***Corresponding Author**
E-mail: syoh@sm.ac.kr
Tel: +82-2-710-9563, Fax: +82-2-710-9871

the controllable surface functionalities make them as an excellent candidate for drug carrier. Drug molecules can be physically entrapped inside the cavity space of the dendrimer or form a conjugate by covalent bond with the functional group on the surface (Liu and Fréchet, 1999; Zhu and Shi, 2013).

There have been a number of literatures using dendrimers as a transdermal enhancer by passive diffusion (Sun *et al*., 2012). Dendrimers increased the skin penetration of both lipophilic and hydrophilic drugs. The steady state flux of indomethacin increased significantly with PAMAM dendrimer at 0.2% (w/v) dendrimer concentration (Chauhan *et al*., 2003). The skin permeation of 5-fluorouracil from lipophilic vehicles containing PAMAM dendrimer increased by increasing transepidermal water loss and by decreasing skin resistance (Venuganti and Perumal, 2008). The influence of surface charge, generation and concentration of PAMAM dendrimers on skin permeation has been studied and the results showed that lower generation cationic dendrimer is more effective in enhancing the skin permeation of hydrophilic drugs (Venuganti and Perumal, 2009). However, the employment of active permeation enhancement method like iontophoresis together with dendrimer is shallow in literature, although PAMAM dendrimer can be a very useful drug carrier, due to its strong positive surface charge and high entrapment of drug molecules inside a single dendrimer molecule (Abla *et al*., 2005). Transdermal delivery of peptide dendrimers by iontophoresis significantly increased the permeation of all the tested peptide dendrimers across human skin in a molecular weight-dependent manner compared to simple passive diffusion (Mutalik *et al*., 2013). They concluded that electromigration was the dominant mechanism for the iontophoretic permeation enhancement. In another study, iontophoretic skin penetration of PAMAM dendrimer as a function of surface charge and molecular weight has been studied using FITC-labeled dendrimers and CLSM (Venuganti *et al*., 2011). Their results demonstrated that cationic dendrimers showed higher penetration than neutral and anionic dendrimers, and the penetration was inversely related to their molecular weight. They showed that dendrimer penetrated the skin through intercellular and hair follicular region.

The aim of this work is to further investigate the effect of PAMAM dendrimer on EOF through skin. Because the surface of PAMAM dendrimer has strong positive charges, it may serve as a good drug carrier for iontophoretic delivery by electromigration. However, because the total flux through skin can also be affected by EOF, the evaluation of this effect is also necessary for better understanding of iontophoretic transport of dendrimer with entrapped or conjugated drug molecules. In fact, it has been reported that, unlike small molecules, the macromolecules are mainly transported by EOF (Guy *et al*., 2000). When dendrimer molecules are transported into CCP of skin, these molecules may interact with the opposite charge on the wall of CCP. This interaction may neutralize or even reverse the charge of the pore wall of CCP. The reversion in charge can lead to the change in the direction and magnitude of EOF. The effect on the quantity and direction of EOF has been examined, using charged polypeptides, such as poly(L-lysines) and poly(L-glutamic acids) (Hirvonen and Guy, 1998). Their results showed that electrotransport of cationic poly(L-lysines) attenuated EOF in the normal anode-to-cathode direction; the degree of inhibition was correlated both with the initial concentration of poly(L-lysine) and with the molecular weight of the polypeptide employed (from 1 to 25 KDa). One interesting aspect of PAMAM dendrimer is its shape. Poly (L-lysines) is a linear chain polyelectrolyte which have a random coil conformation in aqueous solution at neutral pH. However, the PAMAM dendrimer is a spherically shaped polyelectrolyte. This difference in shape may exhibit some difference in their ability to penetrate into CCP and interact with the surface charges in CCP.

In this work, the effect of size and concentration of dendrimer on EOF was studied. The change in EOF was studied using conventional *in-vitro* iontophoresis methodology. As a marker molecule for the direction and magnitude of EOF, a neutral molecule, AAP (pKa=9.86 ± 0.13, M.W.=151.2,) was used. The effect of methanol used for the preparation of aqueous dendrimer solution was also studied, because organic solvent can alter the magnitude of EOF (Lee *et al*., 2014). Finally, we studied the transport of dendrimer into CCP of skin using CLSM. G4 dendrimer with covalently bound FITC was introduced into the diffusion cell and was transported into the skin by iontophoresis or passive diffusion. CLSM study of free FITC was also made for comparison, after free FITC was transported into skin by iontophoresis or passive diffusion.

MATERIALS AND METHODS

Materials

All reagents and chemicals were of the highest commercially obtainable purity. AAP, HEPES (N-[2-hydroxyethyl]-piperazine-N0-12-ethane sulfonic acid) and PTFE filter (0.45 μm) were purchased from Sigma-Aldrich Chemical Co (St. Louis, MO, USA). PAMAM dendrimers (G1, G4 and G7) were obtained from Aldrich Chemical Co (Milwaukee, WI, USA). FITC (Isomer I) by Molecular Probes™ (Carlsbad, CF, USA) was purchased from Interscience (Seoul, Korea). Methanol (HPLC grade) was supplied by Duksan Chemical Co (Seoul, Korea). Side-by-side diffusion cell was custom-made by Yuil Science (Busan, Korea). Ag/AgCl electrode was used for their stability and reversibility. The rod-shaped electrodes were prepared by dipping the tip of an Ag wire (99.9%; Aldrich, Milwaukee, WI, USA) (1 mm diameter) into the molten AgCl. TLC plate (silica gel) was obtained from Merck KGaA (Darmstadt, Germany). Dialysis tubing (molecular weight cutoff 3500) was supplied from Koma Biotechnology Co (Seoul, Korea). Instruments used were power supply (Model PT 70-10 MDC, Powertech, An-San, Korea), HPLC (Shimadzu CBM10A, Tokyo, Japan) and incubator (SI-900, Jeio Tech, Kimpo, Korea). HEPES buffer solutions were prepared using distilled and deionized water from Nanopure ultrapure water system (Barnstead, Iowa, USA). CLSM study was made using FLUOVIEW-FV 300 (Inverted microscope IX71) by Olympus (Tokyo, Japan).

Transport experiment by iontophoresis

AAP transport experiment through skin was performed using full-thickness hairless mouse skin. The skin was excised and frozen immediately after sacrifice of 8 week old hairless mouse (Orient Co., Seoul, Korea). It was stored at -70°C and thawed just before use. A side-by-side diffusion cell was used. The skin was mounted on side by-side diffusion cell with the stratum corneum (SC) side facing the donor chamber. The area of skin exposed to each chamber was 0.5 cm^2. The diffusion chamber held a volume of 1.0 mL and was magnetically stirred. AAP was delivered by anodal (anode placed in

Table 1. The molecular weight, diameter and the number of surface primary amine group of the three dendrimers used (Sharma *et al*., 2005)

Dendrimer	Molecular weight (Da)	Diameter (nm)	Number of surface primary amines
G1	1,430	2.2	8
G4	14,215	4.5	64
G7	116,493	8.1	512

donor chamber) or cathodal (cathode placed in donor chamber) iontophoresis. Transport by simple diffusion (passive) was also studied. Constant current of 0.6 mA/cm^2 was applied continuously to Ag/AgCl electrode mounted on diffusion cell at 32.5°C. The donor chamber was filled with 25 mM HEPES and 133 mM NaCl buffered solution (pH 7.4) containing AAP (10 mg/ml) and PAMAM dendrimer. The receptor chamber was filled with the same buffer solution without AAP and PAMAM dendrimer. At a predetermined time intervals, samples were obtained from receptor chamber and an equal volume of same buffer solution was added. The concentrations of PAMAM dendrimer studied were 7.0×10^{-6} M, 3.5×10^{-5} M and 7.0×10^{-5} M. Dendrimer aqueous solution was prepared by dilution of methanol solution of dendrimer with the same buffer solution above. Three PAMAM dendrimers with different molecular weight (G1, G4 and G7) were studied for their effect on EOF. Table 1 shows the molecular weight, diameter and the number of surface primary amine group for the three dendrimers used (Sharma *et al*., 2005).

AAP assay

The concentration of AAP in receptor chamber was analyzed by a high-performance liquid chromatography (HPLC) system using a Shimadzu CBM-10A system and a SIL-10A auto injector at a wavelength of 295 nm. The column and guard column used were Spherisorb® 10 μm ODS$_2$, 4.6×250 mm and Bondapak™ 10 μm 125 Å C18 (Waters, Miliford, MA, USA), respectively. The mobile phase used for HPLC consisted of methanol-deionized water (40:60). Flow rate was 1.2 ml/min.

Preparation of G4-FITC

For the visualization of the penetration and distribution of G4 dendrimer across the skin, they were labeled with FITC. Covalent linkage between the amine group of G4 dendrimer and the isothiocyanate group of FITC was made by the following method (Jevprasesphant *et al*., 2003). A methanol solution of FITC was added slowly into phosphate-buffered saline (PBS, pH 9.0) containing dendrimer at room temperature and incubated for 24 hours in the dark. The molar ratio of G4 dendrimer to FITC in the mixture was 1.0:1.2. Unreacted FITC was separated by dialysis against distilled water using dialysis tubing (molecular weight cutoff 3500) until free FITC could not be detected by thin-layer chromatography. The mobile phase for TLC was composed of chloroform, methanol and ammonia in the ratio of 5:4:1.

CLSM assay

Using conventional *in-vitro* iontophoresis methodology, the skin penetration of G4-FITC was performed. The donor chamber was filled with the G4-FITC solution and the receptor chamber was filled with PBS (pH 9.0) only. The dendrimer-FITC conjugate was delivered into skin by anodal (anode placed in donor chamber) and cathodal (cathode placed in donor chamber) iontophoresis, using a constant current (0.6 mA/cm^2). Transport by simple diffusion (passive) was also studied. Continuous direct current was applied for an hour to Ag/AgCl electrode mounted in the cell using a power supply. Experiments were conducted at 32.5°C. To study the skin distribution of FITC labeled dendrimer, confocal images were first obtained in the xy plane (parallel to the skin surface) by taking a series of optical sections at successive focal planes along the z axis. The skin surface was then taken as the plane with brightest fluorescence and SC surface morphology. To generate an xz-section, a horizontal line was drawn across a region of interest on the skin surface (Z=0 μm xy-plane) and then optically sliced through the image of successive xy-sections. The xz section images were obtained by optical sectioning from the skin surface at a step size of 1 μm/scan. CLSM study of free FITC was also made for comparison. Experiments were carried out at 100 magnifications.

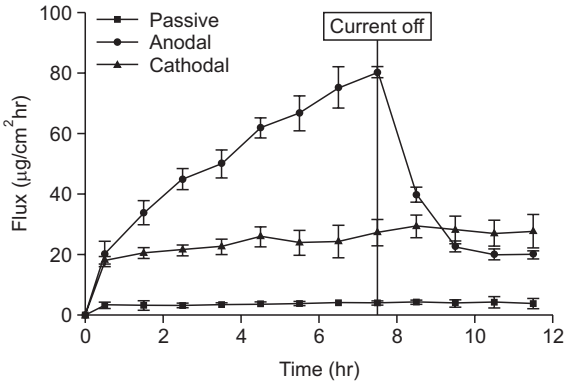

Fig. 1. The effect of electrode polarity on AAP flux across hairless mouse skin *in vitro*. Current was applied for 8 hours with a current density of 0.6 mA/cm^2. Passive delivery is also shown. HEPES buffer solution (pH 7.4) containing 10 mg/ml AAP was used as the donor solution. Each data point represents the mean (± SD) of three experiments.

RESULTS

The effect of EOF on AAP flux

Fig. 1 shows the anodal, cathodal and passive flux of AAP without dendrimer in donor solution. Passive flux was very small and was less than 5 μg/cm^{2}h. Anodal flux increased gradually with time until the current was off. The highest flux obtained was 80 μg/cm^{2}h just before current off. After current off, AAP flux decreased rapidly and reached a plateau value (~20 μg/cm^{2}h). Cathodal flux was ~20 μg/cm^{2}h during current application. This value is much smaller than that observed for anodal delivery during current application. After current off, flux increased slightly and reached a plateau value (28 μg/cm^{2}h). In both anodal and cathodal delivery, the plateau value was 5-7 times larger than that of passive delivery.

The effect of dendrimer size and concentration on EOF

Anodal, cathodal and passive flux of AAP are shown in Fig. 2A, when G1 dendrimer is contained in donor solution at a

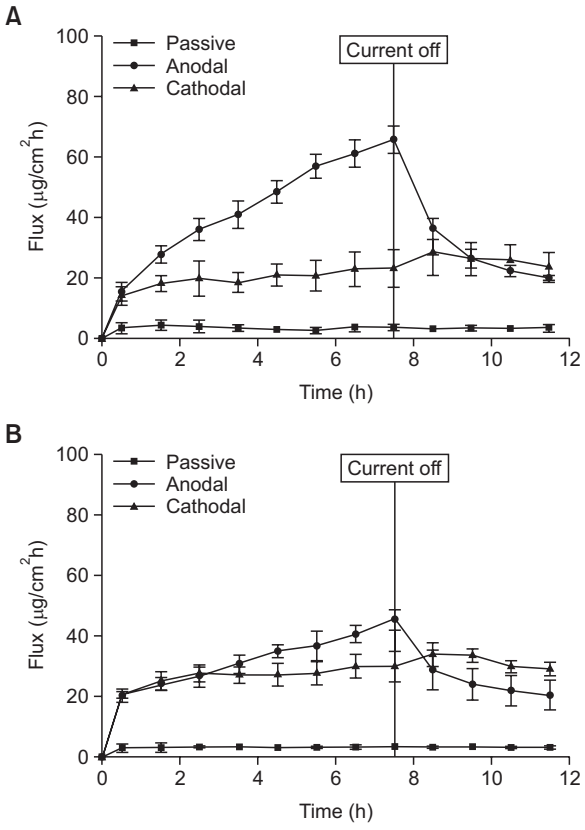

Fig. 2. The effect of G1 dendrimer on anodal, cathodal and passive flux of AAP across hairless mouse skin *in vitro*. HEPES buffer solution (pH 7.4) containing 10 mg/ml AAP and G1 dendrimer at a concentration of (A) 3.5×10^{-5} M or (B) 7.0×10^{-5} M was used as the donor solution. Current was applied for 8 hours with a current density of 0.6 mA/cm^2. Each data point represents the mean (± SD) of three experiments.

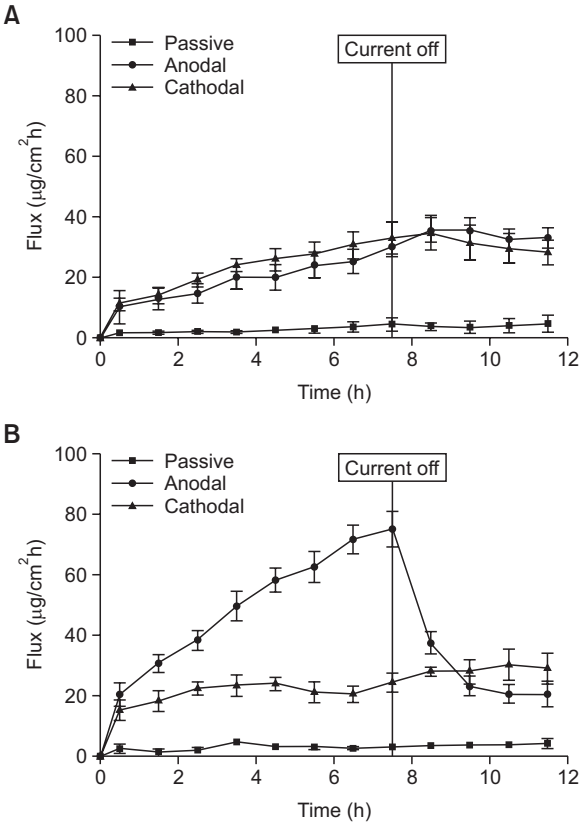

Fig. 3. The effect of G4 dendrimer and methanol on anodal, cathodal and passive flux of AAP across hairless mouse skin *in vitro*. The donor solution was (A) HEPES buffer solution (pH 7.4) with G4 dendrimer (3.5×10^{-5} M) and methanol (0.6% (w/w)) or (B) the same solution without dendrimer. Current was applied for 8 hours with a current density of 0.6 mA/cm^2. Each data point represents the mean (± SD) of three experiments.

concentration of 3.5×10^{-5} M. Anodal flux increased gradually with time until the current was off. The highest flux obtained was 66 μg/cm²h just before current off. After current off, AAP flux decreased rapidly and reached a plateau value. Cathodal flux showed similar values as those obtained without dendrimer (Fig. 1). After current off, flux slightly increased and reached a plateau value (~26 μg/cm²h). Passive flux of AAP was also similar to that obtained in Fig. 1. When the concentration of dendrimer increased further to 7.0×10^{-5} M (Fig. 2B), similar pattern in anodal flux was observed, but the degree in flux increase during current application was much smaller than that observed for 3.5×10^{-5} M (Fig. 2A). The highest flux obtained was 45 μg/cm²h just before current off. After current off, AAP flux decreased rapidly and reached a plateau value similar to that obtained in Fig. 1.

Fig. 3A shows the anodal, cathodal and passive flux of AAP with G4 dendrimer in donor solution (3.5×10^{-5} M). Anodal flux decreased remarkably, when compared to the flux obtained for G1 dendrimer at the same concentration (Fig. 2A). Anodal flux seemed to be even smaller than the cathodal flux during current application and it increased slightly after current off. Cathodal flux showed similar values as those observed above (Fig. 1), indicating that the effect of dendrimer is negligible. Passive flux of AAP was also similar to that observed in Fig. 1. Fig. 3B shows the AAP flux from the HEPES buffer solution used for Fig. 3A, but without dendrimer. This solution contained a low concentration of methanol (0.6% (w/w)), which was originated from the G4 dendrimer stock solution. This study was carried out to evaluate the effect of methanol on EOF, because organic solvent can alter the magnitude of EOF (Lee *et al*., 2014). This evaluation was necessary to assess the relative contribution of dendrimer and methanol on the decrease in EOF. Passive and cathodal flux showed similar magnitude of flux to that observed in Fig. 1, indicating that the methanol effect was negligible. However, in anodal delivery, there was a slight decrease in flux during current application (Fig. 3B), when compared to that observed for buffer solution without methanol (Fig. 1). The maximum anodal flux obtained was 75 μg/cm²h just before current off. After current off, flux decreased rapidly and reached a plateau value similar to that obtained in Fig. 1.

Anodal, cathodal and passive flux of AAP are shown in Fig. 4A, when G7 dendrimer was contained in donor solution at a concentration of 7.0×10^{-6} M. Anodal flux decreased remarkably, when compared to the anodal flux obtained for G1 and G4 dendrimers (Fig. 2A, 3A). Anodal flux was even smaller than the cathodal flux during current application. The direction of EOF during current application seemed to be reversed,

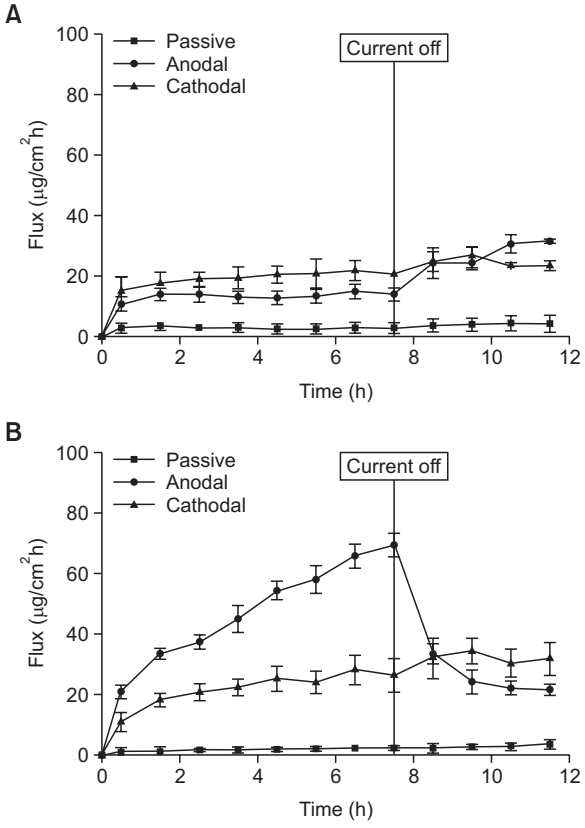

Fig. 4. The effect of G7 dendrimer and methanol on passive, anodal and cathodal flux of AAP across hairless mouse skin *in vitro*. The donor solution was (A) HEPES buffer solution (pH 7.4) with G7 dendrimer (7.0×10^{-6} M) and methanol (2.0% (w/w)) or (B) the same solution without dendrimer. Current was applied for 8 hours with a current density of 0.6 mA/cm^2. Each data point represents the mean (± SD) of three experiments.

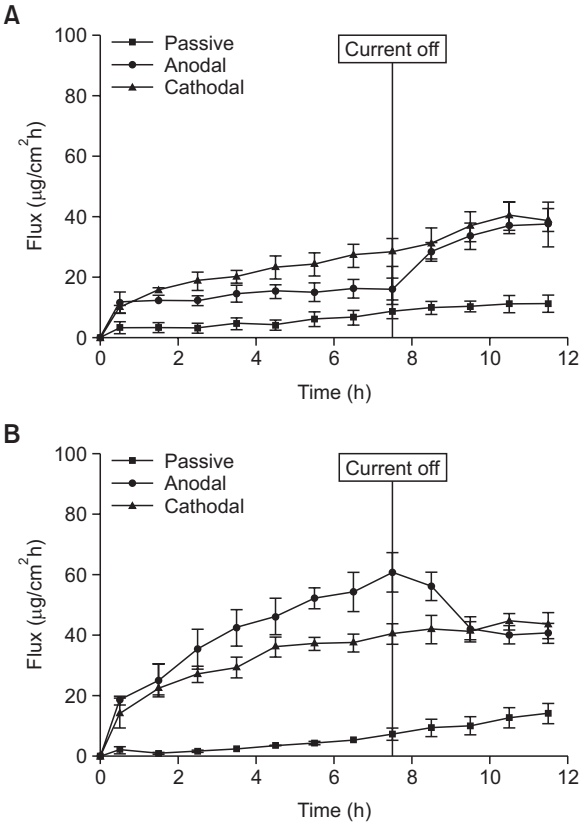

Fig. 5. The effect of G7 dendrimer and methanol on anodal, cathodal and passive flux of AAP across hairless mouse skin *in vitro*. The donor solution was (A) HEPES buffer solution (pH 7.4) with G7 dendrimer (3.5×10^{-5} M) and methanol (10% (w/w)) or (B) the same solution without dendrimer Current was applied for 8 hours with a current density of 0.6 mA/cm^2. Each data point represents the mean (± SD) of three experiments.

as indicated by the increase in flux after anodal current off. Cathodal and passive flux showed similar values as those observed above in Fig. 1. Fig. 4B shows the anodal, cathodal and passive flux of AAP from solution used for above study (Fig. 4A), but without dendrimer. This solution contained 2.0% (w/w) methanol, which is originated from the G7 dendrimer stock solution. Methanol decreased the anodal flux further than that observed in Fig. 3B during current application. The maximum anodal flux obtained was 69 μg/cm²h just before current off. Passive and cathodal flux showed similar magnitude and pattern of flux as observed in Fig. 1, indicating that the methanol effect was minimal.

Fig. 5A shows the anodal, cathodal and passive flux of AAP with G7 dendrimer in donor solution at a concentration of 3.5×10^{-5} M. Anodal delivery showed a similar magnitude in flux to that observed in Fig. 4A. It was smaller than the cathodal flux during current application. Passive and cathodal flux increased considerably with time. Fig 5B shows the flux of AAP from aqueous solution used for above study (Fig. 5A), but without dendrimer. This solution contained a high concentration of methanol (10% (w/w)), which was originated from the G7 dendrimer stock solution. The passive and cathodal flux increased notably, when compared to those observed in Fig. 4B. However, anodal flux decreased further during current application, when compared to that from Fig. 4B. The maximum flux obtained was 61 μg/cm²h just before current off. The passive flux after anodal current off was about two fold larger than that observed in Fig. 4B.

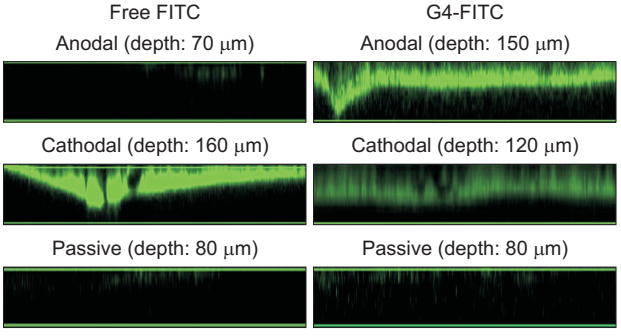

Fig. 6. CLSM images of hairless mouse skin after 1 hour of anodal and cathodal iontophoresis (0.6 mA/cm^2) of free FTIC and G4-FITC. The passive application was also studied. Images were taken in xz plane from surface to 70-160 μm in skin, depending on the experiment.

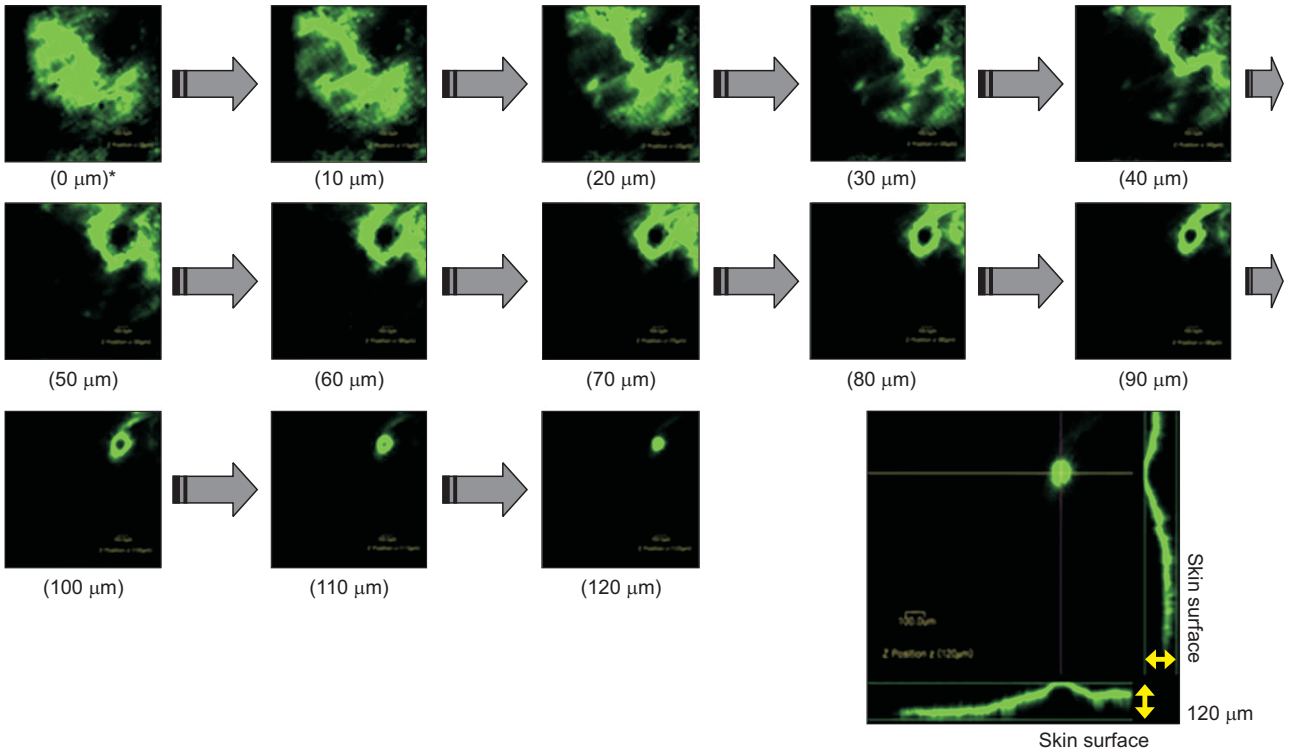

Fig. 7. CLSM images of excised hairless mouse skin after 1 hour anodal iontophoresis (0.6 mA/cm^2) of G4-FITC from top (SC side) to bottom (dermis side). Images represent sequential scans in xy plane from 0 (skin surface) to 120 μm in 10 μm increment. The last image shows the xz and yz plane from surface to 120 μm, together with the xy plane image at 120 μm. The xz and yz scan was taken at the position of line drawn on the bright spot at 120 μm xy plane image.

Skin penetration of G4-FITC

G4-FITC was prepared by previously described method (Jevprasesphant *et al*., 2003). This method reported to prepare a G4-FITC with an average molar ratio of 1:1. Anodal, cathodal and passive application were carried out for 1 hour using free FITC and G4-FITC. The xz optical sections of hairless mouse skin are shown in Fig. 6. Images were taken in xz plane from surface to 70-160 μm in skin. Passive delivery of free FITC showed no fluorescence of FITC from epidermis and dermis region (0-80 μm in depth from the surface). Extremely faint fluorescence from epidermis region could barely be noticed sporadically. Anodal delivery of free FITC showed no fluorescence in skin at all. Strong fluorescence was observed from the surface of SC to dermis region, when free FITC was delivered by cathodal iontophoresis. Cathodal delivery of free FITC showed strong fluorescence in epidermis and dermis region. For G4-FITC, passive delivery showed very similar shape in fluorescence to that of free FITC. Fluorescence after passive delivery was extremely faint and sparsely observed across the skin. Anodal delivery showed strong fluorescence and the G4-FITC was densely distributed from the surface of SC to dermis region. When the conjugate was delivered by cathodal iontophoresis, fluorescence was observed as deep as dermis, similar to the result for anodal delivery. However, the intensity of fluorescence was very weak.

Fig. 7 shows the z series parallel CLSM images of FITC-labeled G4 dendrimer from top (SC side) to bottom (dermis side) after 1 hour anodal iontophoresis. Images represent sequential scans in xy plane from 0 (skin surface) to 120 μm in 10 μm increment. The last image shows the xz and yz plane from surface to 120 μm, together with the xy plane image at 120 μm. The xz and yz scan was taken at the position of line drawn on the bright spot at 120 μm xy plane image. From surface (0 μm) to 30 μm (probably the SC and the viable epidermis region), the fluorescence of G4-FITC was diffused on the xy plane. After 30 μm in depth, it seems that the fluorescence is limited around a black spot, which seems to be a hair shaft. The last xy plane image at 120 μm showed no black spot in the middle, indicating that the G4-FITC reached the hair bulb region.

DISCUSSION

Fig. 1 shows AAP flux during iontophoresis. Because AAP is not charged at the experimental condition, there is no flux contribution by electromigration. Only EOF and passive diffusion can contribute to the flux. Hence, the gradual increase in flux during anodal current application is due to the combined effect of EOF and permeability increase by structural changes of SC (Pikal, 2001). Because the direction of EOF is from anode to cathode, there is a flux enhancement effect by EOF when anodal current is applied. From the difference in anodal flux immediately before (80 μg/cm^{2}h) and after current off (40 μg/cm^{2}h), the magnitude of EOF was estimated to be about 4.0 μl/cm^{2}h, by dividing the difference in electrotransport of AAP by its concentration in the donor solution. This value is comparable to the values in literature for hairless mouse (2.0-4.2 μl/cm^{2}h) (Marro *et al*., 2001; Lee *et al*., 2014). The

increase in flux after cathodal current off is probably due to the disappearance of flux impeding effect by EOF and to the increase in passive permeability by current induced structural changes of SC (Lee and Oh, 2005; Lee *et al*., 2014).

When G1 dendrimer was added to the donor solution at a concentration of 3.5×10^{-5} M (Fig. 2A), flux increase during anodal current application was slightly smaller than that observed without dendrimer (Fig. 1). It became even smaller as the concentration of dendrimer increased further to 7.0×10^{-5} M (Fig. 2B). This seems to be related to the decrease in EOF by the interaction between the negative charge of CCP and G1 dendrimer that migrated into CCP. This leads to a subsequent loss of skin permselectivity and an attenuation of EOF in conventional anode-to-cathode direction. No effect of dendrimer on cathodal flux was observed. This is probably due to the electroattraction of cationic PAMAM dendrimer molecules by cathode, and thus, dendrimer molecules do not move into CCP.

When G4 dendrimer was added to the donor solution at a concentration of 3.5×10^{-5} M (Fig. 3A), anodal flux decreased remarkably, and the direction of EOF during current application seemed to be reversed slightly, as indicated by the increase in flux after anodal current off. These results seem to be related to the higher positive surface charge of G4 dendrimer (64 surface charges) than G1 dendrimer (8 surface charges). Hence, the association of G4 dendrimers with CCP can lead to a charge inversion to a net positive charge. This can reverse the direction of EOF, as shown in anodal flux data. The effect of dendrimer on cathodal and passive delivery was negligible, probably due to the difficulty in skin permeation of dendrimer. It has been shown that G4 dendrimers were mainly limited to SC after passive application (Venuganti *et al*., 2011). The slight decrease in anodal AAP flux by methanol (Fig. 3B) is probably due to the decrease in EOF. The increase in solution viscosity (Kubota *et al*., 1980) and the decrease in solution dielectric constant (Megriche *et al*., 2012) seem to be the main reason for this decrease in EOF as described by the Helmholtz–Smoluchowski equation (Pamukcu and Wittle, 1992),

$$V_{eo} = \frac{\varepsilon\zeta}{\eta} E$$

where v_{eo}, ζ, ε, η and E are the bulk phase electroosmotic fluid velocity, zeta potential, dielectric constant of the fluid, viscosity of the fluid and the applied electric field strength, respectively. If this decrease in EOF by methanol was excluded in Fig. 3A, the anodal AAP flux during current application might have been slightly higher. However, the magnitude of decrease in EOF by methanol is much smaller, when compared to that by G4 dendrimer.

The anodal flux with G7 dendrimer in donor solution (Fig. 4A) showed a remarkable decrease and the direction of EOF seemed reversed. G7 dendrimer has much higher positive surface charge (512 surface charges) than G4 dendrimer (64 surface charges). The reversal in the direction of EOF strongly suggests that these G7 macromolecules were driven into CCP, resulting in the reversal in net charge of CCP. Presumably, the large size and subsequent slower permeability of G7 dendrimer macromolecule resulted in a significant association with CCP during current passage. Actually the concentration of G7 dendrimer in Fig. 4A is only 1/5 of the concentration studied for the G1 and G4 dendrimer (Fig. 2A, 3A). Fig. 3B shows the effect of methanol on flux at the concentration of 2.0 % (w/w). Methanol at this concentration decreased the anodal flux further than that observed in Fig. 3A during current application, indicating that the magnitude of EOF decreased further by the increased methanol concentration. However, the magnitude of decrease in EOF by methanol seems much smaller than that by dendrimer (Fig. 4A).

When the concentration of G7 dendrimer increased to 3.5×10^{-5} M, considerable increases in passive and cathodal flux were observed for both solutions with and without dendrimer (Fig. 5A, 5B). These results indicate that methanol acted as a skin permeation enhancer at this concentration (10% (w/w)). Anodal flux in Fig. 5A shows that the direction of EOF is reversed. Because the concentration of G7 dendrimer is 5 times higher, the magnitude of flux impeding effect by EOF is expected to be higher than that from 7.0×10^{-6} M solution. Thus, the anodal flux during current application could be expected to be smaller than that observed in Fig. 4A, if only dendrimer effect was considered. However, the anodal flux in Fig. 5A shows a similar magnitude as in Fig. 4A. The reason for this is probably due to the increase in passive permeability by methanol at this concentration, as mentioned above. The anodal flux during current application without dendrimer could also be expected to be smaller than that observed in Fig. 5B, if only the effect of methanol on EOF was considered. Flux enhancing effect by methanol is clearly reflected in the passive flux after anodal current off (Fig. 5B), which is about two fold larger than that observed in Fig. 4B.

The thicknesses of SC and epidermis for hairless mouse skin are reported to be about 10 μm and 30 μm, respectively (Jung and Maibach, 2015). Extremely faint fluorescence of free FITC could be noticed sporadically from epidermis region after passive delivery (Fig. 6). One interesting point is the needle-like shape of this fluorescence. It is unlikely that charged FITC molecules permeate into the intact intercellular domain only by passive diffusion. It seems that free FITC molecules diffused mainly into follicular region. The density of hair follicle in hairless mouse was reported to be 75 ± 6/cm^2 (Bronaugh *et al*., 1982) or 100-150/cm^2 (Scott *et al*., 1995). In another report, the number was 400-500/cm^2, including the rudimentary hair follicles (Yamashita *et al*., 1997). Anodal delivery of free FITC showed no fluorescence in skin, probably due to the electroattraction of negatively charged FITC by anode. The strong fluorescence after cathodal iontophoresis indicates that large amount of free FITC penetrated into skin, probably due to the electrorepulsive force between FITC and cathode. It seems that FITC molecules penetrated into skin through follicular and intercellular region, as previously reported (Venuganti *et al*., 2011). They have shown that, after iontophoresis, cationic G4 dendrimer penetrated into the skin to a depth of 80 μm of porcine SC. Dendrimers were found in the skin furrows, intercellular lipid regions and hair follicles. However, clustered regions of bright fluorescence were also observed. These regions were repeatedly observed only in the iontophoretic treatment group which appears to be localized transport regions for the dendrimer (Venuganti *et al*., 2011). We speculate that these localized regions might be related to new pores created by skin damage of iontophoretic current. It was reported that, after iontophoresis, some unidentified pores (~20 μm in diameter) were observed in the region where no anatomical structure could be seen by optical microscopy (Scott *et al*., 1992).

After anodal iontophoresis of G4-FITC, strong fluorescence was observed from SC to dermis region. This is probably due

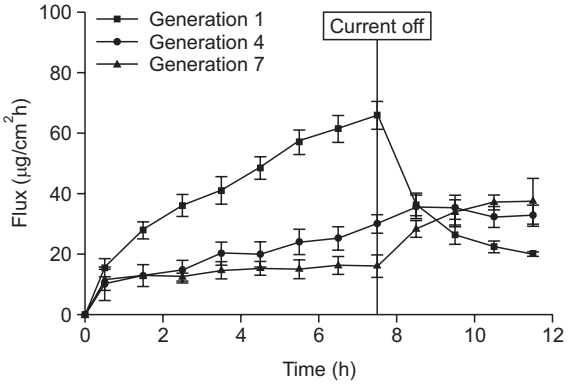

Fig. 8. The effect of PAMAM dendrimer generation on anodal, cathodal and passive flux of AAP across hairless mouse skin *in vitro* (Data from Fig. 2A, 3A, 5A).

to the high positive surface charge density of the dendrimer conjugate. Because the net charge of CCP is expected to be reversed by the G4-FITC, probably the flux of G4-FITC was impeded by EOF, though the magnitude was much smaller than that by electromigration. When the conjugate was delivered by cathodal iontophoresis, fluorescence was observed as deep as dermis. But, the intensity of fluorescence was very weak. Because of the net positive charge, it seems very difficult for G4-FITC to penetrate into the skin by cathodal delivery. It seems reasonable that this faint fluorescence is due to the free FITC molecules which were left over in dialysis sac. Fluorescence after passive delivery of G4-FITC was extremely faint and sparsely observed across the skin. This result indicates that G4-FITC can hardly penetrate the skin, except the follicular region, as discussed above. The image in Fig. 7 reveals that hair follicle is clearly a pathway for G4 dendrimer into the deeper dermal region of skin. A recent study proved that G4 dendrimer can target to the follicles of pig skin by both passive diffusion and iontophoresis, which verified the role of follicular route in the skin penetration of dendrimer (Venuganti *et al*., 2011). The importance of follicular route in nanoparticulate skin delivery has gradually been gaining attention, despite the low density of hair follicles on the skin's surface (<0.1%), (Lademann *et al*., 2007).

Fig. 8 shows the anodal flux of G1, G4 and G7 dendrimers at the concentration of 3.5×10^{-5} M (data from Fig. 2A, 3A, 5A). The effect of each generation on EOF can be seen more clearly. G1 did not change the direction of EOF. In case of G4 and G7, as indicated by the decrease in anodal flux during current application and the increase in flux after current removal, the direction of EOF was reversed to cathode-to-anode direction. This reversal in direction strongly suggests that these macromolecules were driven into CCP, and interacted with the negative charges of CCP. Their large size and high charge densities compensated the original negative surface charge resulting in a net positive surface charge. G7 dendrimer which is larger in size and the number of surface charge showed stronger reversal in EOF than G4 dendrimer. It seems that the ability to migrate into CCP is higher for spherical dendrimer molecule than linear polyelectrolyte, because the hydrodynamic size for spherical dendrimer is much smaller than the linear polyelectrolyte with same molecular weight. Poly(L-lysines) transport study has shown that iontophoresis greatly enhanced the penetration of the 4 KDa analog, slightly elevated the delivery of the 7 KDa FITC-PLL, but had no effect on the transport of the larger 26 KDa FITC- poly(L-lysines) (Turner *et al*., 1997). However, the data obtained in this work have shown that G7 dendrimer with much higher molecular weight (Mw. 116,493) than 26 KDa FITC- poly(L-lysines) can migrate into CCP under current.

In conclusion, this work showed that PAMAM dendrimers can migrate into the CCP of skin and modulate the EOF through skin by iontophoresis. The results seem to indicate that the larger size of G4 and G7, and accompanying larger number of surface positive charge resulted in slower movement of these macromolecules in CCP, leading to a strong interaction with the net negatively charged CCP during permeation. This interaction seemed to invert the charge of CCP to a net positive charge, and reversed the direction of EOF from the normal anode-to-cathode direction to cathode-to-anode direction. G7 dendrimer exhibited stronger reversal in EOF than G4 dendrimer. G1 dendrimer seemed to weaken the EOF, but did not change the direction of EOF at the concentration range studied. Cross-sectional view perpendicular to the skin surface by confocal microscopy study showed that G4-FITC could penetrate into the viable epidermis and dermis area under anodal current. The permeation route seemed to be mainly localized on follicular region. Overall, we obtained a better understanding on the mechanistic insights into the electroosmosis phenomena and its role on flux during iontophoresis.

CONFLICT OF INTEREST

All authors declare that they have no conflict of interest.

ACKNOWLEDGMENTS

This Research was supported by the Sookmyung Women's University Research Grants 2014.

REFERENCES

Abla, N., Naik, A., Guy, R. H. and Kalia, Y. N. (2005) Effect of charge and molecular weight on transdermal peptide delivery by iontophoresis. *Pharm. Res.* **22**, 2069-2078.

Bronaugh, R. L., Stewart, R. F. and Congdon, E. R. (1982) Methods for *in vitro* percutaneous absorption studies. II. Animal models for human skin. *Toxicol. Appl. Pharmacol.* **62**, 481-488.

Burnette, R. R. and Ongpipattanakul, B. (1987) Characterization of the permselective properties of excised human skin during iontophoresis. *J. Pharm. Sci.* **76**, 765-773.

Chauhan, A. S., Sridevi, S., Chalasani, K. B., Jain, A. K., Jain, S. K., Jain, N. K. and Diwan, P. V. (2003) Dendrimer-mediated transdermal delivery: Enhanced bioavailability of indomethacin. *J. Control. Release* **90**, 335-343.

Choudhary, S., Gupta, L., Rani, S., Dave, K. and Gupta, U. (2017) Impact of dendrimers on solubility of hydrophobic drug molecules. *Front. Pharmacol.* **8**, 261.

Esfand, R. and Tomalia, D. A. (2001) Poly(amidoamine) (PAMAM) dendrimers: from biomimicry to drug delivery and biomedical applications. *Drug Discov. Today* **6**, 427-436.

Guy, R. H., Kalia, Y. N., Delgado-Charro, M. B., Merino, V., Lopez, A. and Marro, D. (2000) Iontophoresis: electrorepulsion and electroosmosis. *J Control. Release* **64**, 129-132.

Hirvonen, J. and Guy, R. H. (1998) Transdermal iontophoresis: modulation of electroosmosis by polypeptide. *J Control. Release* **50**, 283-289.
Jevprasesphant, R., Penny, J., Attwood, D., McKeown, N. B. and D'Emanuele, A. (2003) Engineering of dendrimer surfaces to enhance transepithelial transport and reduce cytotoxicity. *Pharm. Res.* **20**, 1543-1550.
Jo, J. and Oh, S. (2010) Electrotransport of levodopa through skin: permeation at low pH. *J. Pharm. Invest.* **40**, 23-31.
Jung, E. C. and Maibach, H. I. (2015) Animal models for percutaneous absorption. *J. Appl. Toxicol.* **35**, 1-10.
Kim, A., Green, P. G., Rao, G. and Guy, R. H. (1993) Convective solvent flow across the skin during iontophoresis. *Pharm. Res.* **10**, 1315-1320.
Kubota, H., Tsuda, S., Murata, M., Yamamoto, T., Tanaka, Y. and Makita, T. (1980) Specific volume and viscosity of methanol-water mixtures under high pressure. *Rev. Phys. Chem. Jpn.* **49**, 59-69.
Lademann, J., Richter, H., Teichmann, A., Otberg, N., Blume-Peytavi, U., Luengo, J., Weiss, B., Schaefer, U. F., Lehr, C. M., Wepf, R. and Sterry, W. (2007) Nanoparticles-an efficient carrier for drug delivery into the hair follicles. *Eur. J. Pharm. Biopharm.* **66**, 159-164.
Lee, J. H. and Oh, S. (2005) Current pretreatment of skin and its effect on the permeability. *J. Pharm. Investig.* **35**, 81-87.
Lee, S. Y., Jeong, N. Y. and Oh, S. (2014) Modulation of electroosmosis and flux through skin: effect of propylene glycol. *Arch. Pharm. Res.* **37**, 484-493.
Liu, M. and Fréchet, J. M. (1999) Designing dendrimers for drug delivery. *Pharm. Sci. Technol. Today* **2**, 393-401.
Marro, D., Guy, R. H. and Delgado-Charro, M. B. (2001) Characterization of the iontophoretic permselectivity properties of human and pig skin. *J. Control. Release* **70**, 213-217.
Megriche, A., Belhadj, A. and Mgaidi, A. (2012) Microwave dielectric properties of binary solvent wateralcohol, alcohol-alcohol mixtures at temperatures between -35°C and +35°C and dielectric relaxation studies. *Mediterr. J. Chem.* **1**, 200-209.
Mutalik, S., Parekh, H. S., Anissimov, Y. G., Grice, J. E. and Roberts, M. S. (2013) Iontophoresis-mediated transdermal permeation of peptide dendrimers across human epidermis. *Skin Pharmacol. Physiol.* **26**, 127-138.
Niu, Y., Sun, L. and Crooks, R. M. (2003) Determination of the intrinsic proton binding constants for poly(amidoamine) dendrimers via potentiometric pH titration. *Macromolecules* **36**, 5725-5731.
Pamukcu, S. and Wittle, J. K. (1992) Electrokinetic removal of selected heavy metals from soil. *Environ. Prog.* **11**, 241-250.
Pikal, M. J. (2001) The role of electroosmotic flow in transdermal iontophoresis. *Adv. Drug Deliv. Rev.* **46**, 281-305.
Scott, E. R., White, H. S. and Phipps, J. B. (1992) Direct imaging of ionic pathways in stratum corneum using scanning electrochemical microscopy. *Solid State Ion.* **53-56**, 176-183.
Scott, E. R., Phipps, J. B. and White, H. S. (1995) Direct imaging of molecular transport through skin. *J. Invest. Dermatol.* **104**, 142-145.
Sharma, A., Rao, M., Miller, R. and Desai, A. (2005) Fluorometric assay for detection and quantitation of polyamidoamine dendrimers. *Anal. Biochem.* **344**, 70-75.
Sun, M., Fan, A., Wang, Z. and Zhao, Y. (2012) Dendrimer-mediated drug delivery to the skin. *Soft Matter* **8**, 4301-4305.
Tripathy, W. and Das, M. K. (2013) Dendrimers and their applications as novel drug delivery carriers. *J. Appl. Pharm. Sci.* **3**, 142-149.
Turner, N. G., Ferry, L., Price, M., Cullander, C. and Guy, R. H. (1997) Iontophoresis of poly-L-lysines: the role of molecular weight? *Pharm. Res.* **14**, 1322-1331.
Venuganti, V. K. and Perumal, O. P. (2008) Effect of poly(amidoamine) (PAMAM) dendrimer on skin permeation of 5-fluorouracil. *Int. J. Pharm.* **361**, 230-238.
Venuganti, V. K. and Perumal, O. P. (2009) Poly(amidoamine) dendrimers as skin penetration enhancers: Influence of charge, generation, and concentration. *J. Pharm. Sci.* **98**, 2345-2356.
Venuganti, V. V., Sahdev, P., Hildreth, M., Guan, X. and Perumal, O. (2011) Structure-skin permeability relationship of dendrimers. *Pharm. Res.* **28**, 2246-2260.
Yamashita, N., Tachibana, K., Ogawa, K., Tsujita, N. and Tomita, A. (1997) Scanning electron microscopic evaluation of the skin surface after ultrasound exposure. *Anat. Rec.* **247**, 455-461.
Zhu, J. and Shi, X. (2013) Dendrimer-based nanodevices for targeted drug delivery applications. *J. Matater. Chem. B.* **34**, 4199-4211.